International Journal of Dynamics and Control
https://doi.org/10.1007/s40435-022-01053-w

Impacts of lockdown on the dynamics of forestry biomass, wildlife species and control of atmospheric pollution

Sapna Devi[1] · **Reda Fatma**[1] · **Vinay Verma**[2]

Received: 18 July 2022 / Revised: 22 September 2022 / Accepted: 23 September 2022

Abstract
In this paper, we have formulated and analysed a mathematical model to investigate the impacts of lockdown on the dynamics of forestry biomass, wildlife species and pollution. For this purpose, we have considered a nonlinear system of four ordinary differential equations representing rates of change of the density of forestry biomass, the density of wildlife species, the concentration of pollutants and lockdown. Conditions for the existence, uniqueness and local stability of all equilibria along with the global stability of the interior equilibrium point are derived. Furthermore, conditions that influence the persistence of the system are obtained. By formulating an optimal control problem, the optimal strategies for minimizing the cost of implementation of lockdown as well as the concentration of pollutants are also studied. Numerical simulations are carried out to verify and validate our analytical findings. By this study, we have observed that implementation of lockdown for a sufficient period of time minimizes excessive harvesting of both forestry biomass and wildlife species and the concentration of pollutants in the environment. It is also found that lockdown policy is effective in the optimal control of atmospheric pollution. Therefore, lockdown plays a significant role in the dynamics of forestry biomass, wildlife species and control of pollution in the environment.

Keywords Forestry biomass · Wildlife species · Pollutants · Lockdown · Stability · Persistence · Optimal control

1 Introduction

Lockdown is a restriction policy that imposes on human population to ensure their safety from some major risks. Pandemics and imminent threats are some of the main reasons of lockdown. On April 30, 2009, lockdown was imposed in Mexico due to swine flu [1]. In August 2019, the Indian government implemented lockdown on Jammu and Kashmir by restricting communications and media sources after abrogation of status of state [1]. During COVID-19 pandemic, several countries had imposed lockdown that restrict mobility, trade and other socio-economic activities. On January 23, 2020, the first lockdown during COVID-19 pandemic was implemented in Wuhan, China [2]. On March 24, 2020, Indian government declared complete lockdown for the entire country as a preventive measure against the COVID-19 pandemic in India [3]. During the lockdown period, consumption of fuels by industries, thermal power plants and transportation is restricted. As a consequence, lockdown affects forestry biomass, wildlife species and pollution in different aspects. The paper [3] gives insight into the improvement of air quality due to lockdown, using tools like satellite images of Indian atmosphere and Air quality index calculated by central pollution control board of India. Lockdown can do a miraculous change in environmental conditions. However, lockdown policy cannot be implemented forever as industries cannot be shut for much longer time or vehicular movement cannot be restricted for a long period of time but government can change the patterns and adopt a more effective strategy. This gives an idea that imposition of lockdown can improve environmental conditions and can restore disturbed ecology.

✉ Reda Fatma
redafatma7860@gmail.com

Sapna Devi
sapnamaths@rediffmail.com

Vinay Verma
vinay86verma@gmail.com

[1] Department of Mathematics, University of Allahabad, Prayagraj, Uttar Pradesh 211002, India

[2] Faculty of Mathematical and Statistical Sciences, Institute of Natural Sciences and Humanities, Shri Ramswaroop Memorial University, Lucknow-Deva Road, Barabanki, Uttar Pradesh 225003, India

Published online: 13 October 2022

Forests are one of the most essential components for the survival of human population and wildlife species. Besides providing habitat and livelihood for humans and wildlife species, forests offer watershed protection, prevent soil erosion and mitigate climate change. Vogt *et al.* [4] investigated the importance of forestry biomass for human survival and ecological sustainability. Humans are harvesting forestry biomass for producing electricity, industrial facilities and transport energy. But the aggressive harvesting of forestry biomass from forests is a fundamental threat to the health and productivity of the forest ecosystem. The world's forest area has shrunk from the preindustrial level of 5900 million ha (hectare) to 3999 million ha in 2015 [5,6]. The global forest area decreased from 31.6 % to 30.6 % of total land area between 1990 and 2015 [7]. Dubey *et al.* [8] analysed a mathematical model to see the effects of increased industrialization on forestry biomass. Their study claimed that human population pressure and rapid industrialization may increase the temperature of atmosphere of the earth. Therefore, human population pressure and rapid industrialization are very harmful for forestry biomass. Agarwal *et al.* [9] proposed a mathematical model to study the impacts of industrialization on depletion of forestry biomass and its consequent effects on wildlife species. They observed that increase in industrialization affects forestry biomass adversely, which in turn affects the wildlife species. Many other authors [10–13] investigated the impacts of toxicants, population, industrialization and pollution on forestry biomass. Literatures have also evidenced nonlinear mathematical models that explore harvesting of vegetation biomass and prey–predator [14–19]. In [20], authors found that predator harvesting can maintain the stability of the ecological system by terminating persistent oscillations.

Various kinds of pollutants like NO_2 and CO_2 enter into the environment due to the use of fuels in industrialization, transportation and thermal power plants. All these pollutants negatively affect water, air, vegetation, forestry resources and the land, which in turn affects the survival of wildlife species directly or indirectly [21–23]. All above studies suggest that excessive harvesting of both forestry biomass and wildlife species and increasing concentration of pollutants in the environment are a serious matter of concern. Therefore, aggressive harvesting of both forestry biomass and wildlife species and increasing concentration of pollutants in the environment should be controlled by implementing some policy. Imposition of lockdown can reduce excessive harvesting of both forests and wildlife species and increasing concentration of pollutants in the environment. Misra *et al.* [24] formulated an optimal control problem to investigate the impacts of reforestation as well as time lag between measuring forest data and implementing reforestation efforts on the control of atmospheric concentration of CO_2. Verma *et al.* [25] studied the effects of the genetically modified tree planting on the control of CO_2 level in the atmosphere.

The implementation of lockdown is useful to decrease the concentration of pollutants, but the cost of implementation prevents them from being implemented on broad scale. As a result, implementation strategies that minimize the concentration of pollutants and the cost of implementation of lockdown are preferred. Keeping all these in mind, in this paper, we have proposed a mathematical model considering the density of forestry biomass, the density of wildlife species, the concentration of pollutants and lockdown. To the best of our knowledge, no one has formulated a mathematical model to study the effects of lockdown on the dynamics of forestry biomass, wildlife species and control of pollution in the environment. The model is analysed in regard to boundedness, equilibria, local stability, global stability and persistence. Furthermore, optimal control strategies for minimizing the concentration of pollutants as well as the cost of implementation of lockdown are studied by formulating optimal control problem.

2 Mathematical model

Excessive harvesting of both forestry biomass, wildlife species and atmospheric concentration of pollutants can be reduced by the imposition of lockdown policy. To model this scenario, we consider four dynamic variables, namely forestry biomass $F(t)$, wildlife species $W(t)$, concentration of pollutants $P(t)$ and lockdown $L(t)$ at time $t > 0$. Following assumptions and facts are taken into account in mathematical modelling process:

A(1): The dynamics of forestry biomass and wildlife species are governed by the logistic model.

A(2): The density of forestry biomass decreases due to wildlife species.

A(3): The density of wildlife species decreases due to pollutants and increases with forestry biomass.

A(4): Implementation rate of lockdown is constant, and the rate of ineffectiveness of lockdown is taken to be proportional to lockdown.

A(5): The emission rate of pollutants depends on lockdown, and it decreases with the increase in lockdown.

A(6): The uptake rate of pollutants depends on forestry biomass and pollutants in the atmosphere. Also, it negatively feedbacks into forestry biomass.

A(7): The removal rate of pollutants by sinks other than forests is taken to be proportional to the concentration of pollutants in the atmosphere.

A(8): The decrease in wildlife species caused by pollutants is assumed to be feedback into the concentration of pollutants in the atmosphere.

A(9): Harvesting of both forestry biomass and wildlife species decreases with the implementation of lockdown.

Under the above assumptions, our mathematical model is described by the following set of nonlinear ordinary differential equations:

$$\begin{aligned}
\frac{\mathrm{d}F}{\mathrm{d}t} &= rF\left(1-\frac{F}{K}\right)-\alpha_1 WF-\pi_1\beta_1 FP-h_1(L)F,\\
\frac{\mathrm{d}W}{\mathrm{d}t} &= sW\left(1-\frac{W}{M}\right)+\alpha_2 WF-\beta_2 WP-h_2(L)W,\\
\frac{\mathrm{d}P}{\mathrm{d}t} &= Q(L)-\beta_1 FP+\pi_2\beta_2 WP-\delta_0 P,\\
\frac{\mathrm{d}L}{\mathrm{d}t} &= L_0-\eta L,
\end{aligned} \tag{1}$$

with the initial conditions, $F(0)\geq 0$, $W(0)\geq 0$, $P(0)>0$, and $L(0)\geq 0$.
Here, we take $h_1(L)=h_{0_1}-e_1L$ so that $h_1(0)=h_{0_1}>0$ and $h_1'(L)<0$ for $L>0$. Similarly, we consider $h_2(L)=h_{0_2}-e_2L$ so that $h_2(0)=h_{0_2}>0$ and $h_2'(L)<0$ for $L>0$. Also, we consider $Q(L)=Q_0-Q_1L$. Then, $Q(0)=Q_0>0$ and $Q'(L)<0$ for $L>0$.

Therefore, model (1) becomes

$$\begin{aligned}
\frac{\mathrm{d}F}{\mathrm{d}t} &= rF\left(1-\frac{F}{K}\right)-\alpha_1 WF-\pi_1\beta_1 FP-h_{0_1}F+e_1LF,\\
\frac{\mathrm{d}W}{\mathrm{d}t} &= sW\left(1-\frac{W}{M}\right)+\alpha_2 WF-\beta_2 WP-h_{0_2}W+e_2LW,\\
\frac{\mathrm{d}P}{\mathrm{d}t} &= Q_0-Q_1L-\beta_1 FP+\pi_2\beta_2 WP-\delta_0 P,\\
\frac{\mathrm{d}L}{\mathrm{d}t} &= L_0-\eta L,
\end{aligned} \tag{2}$$

with the initial conditions, $F(0)\geq 0$, $W(0)\geq 0$, $P(0)>0$, and $L(0)\geq 0$.
The parameters of the model system (2) are positive and defined in Table 1.

3 Boundedness of solutions

To analyse the model (2), we need the bounds on dependent variables involved, so we find the region of attraction in the next lemma:

Lemma 3.1 *If* $(\delta_0-\pi_2\beta_2 W_{\max})>0$, *then solutions of system* (2) *are bounded inside a region* Ω *given by*

$$\Omega=\Big\{(F,W,P,T):0\leq F\leq F_{\max},0\leq W\leq W_{\max},$$
$$0<P\leq P_{\max},0\leq L\leq L_{\max}\Big\},$$

where $F_{\max}=\frac{K}{r}(r+e_1L_{\max})$, $W_{\max}=\frac{M}{s}(s+\alpha_2F_{\max}+e_2L_{\max})$, $P_{\max}=\frac{Q_0}{(\delta_0-\pi_2\beta_2W_{\max})}$ *and* $L_{\max}=\frac{L_0}{\eta}$.

Proof From the fourth equation of system (2), we have

$$\frac{\mathrm{d}L}{\mathrm{d}t}=L_0-\eta L.$$

This implies that,

$$\limsup_{t\to\infty} L(t)=\frac{L_0}{\eta}=L_{\max},\ (\text{say}).$$

From the first equation of system (2), we get

$$\frac{\mathrm{d}F}{\mathrm{d}t}\leq F\left(r+e_1L_{\max}-\frac{r}{K}F\right).$$

This gives,

$$\limsup_{t\to\infty} F(t)\leq\frac{K}{r}(r+e_1L_{\max})=F_{\max},\ (\text{say}).$$

Proceeding in a similar manner, the second equation of system (2) gives

$$\frac{\mathrm{d}W}{\mathrm{d}t}\leq W\left(s+\alpha_2F_{\max}+e_2L_{\max}-\frac{s}{M}W\right),$$

which implies that

$$\limsup_{t\to\infty} W(t)\leq\frac{M}{s}(s+\alpha_2F_{\max}+e_2L_{\max})=W_{\max},\ (\text{say}).$$

From the third equation of system (2), we have

$$\frac{\mathrm{d}P}{\mathrm{d}t}\leq Q_0-(\delta_0-\pi_2\beta_2W_{\max})P.$$

This implies that

$$\limsup_{t\to\infty} P(t)\leq\frac{Q_0}{(\delta_0-\pi_2\beta_2W_{\max})}=P_{\max},\ (\text{say}).$$

Here, $P_{\max}>0$, if $(\delta_0-\pi_2\beta_2W_{\max})>0$. This completes the proof of Lemma 3.1. □

Table 1 Model parameters

Parameter	Description
r	Intrinsic growth rate of forestry biomass
s	Intrinsic growth rate of wildlife species
K	Carrying capacity of the environment for the density of forestry biomass
M	Carrying capacity of the environment for the density of wildlife species
α_1	Decrease rate of forestry biomass due to wildlife species
α_2	Growth rate of wildlife species due to forestry biomass
$\pi_1(< 1)$	A proportionality constant that represents the depletion of forestry biomass due to pollutants
$\pi_2(< 1)$	A proportionality constant that represents the growth of pollutants due to wildlife species
β_1	Depletion rate of pollutants in the environment due to increase in the density of forestry biomass
β_2	Depletion rate of wildlife species due to increase in the concentration of pollutants
h_{0_1}	Harvesting rate of forestry biomass in the absence of lockdown
h_{0_2}	Harvesting rate of wildlife species in the absence of lockdown
e_1	Growth rate of forestry biomass due to lockdown
e_2	Growth rate of wildlife species due to lockdown
Q_0	Emission rate of pollutants
Q_1	Depletion rate coefficient of pollutants due to increase in lockdown
δ_0	Natural depletion rate coefficient of pollutants
L_0	Implementation rate of lockdown
η	Rate of ineffectiveness of lockdown

4 Equilibrium analysis

System (2) has following four nonnegative equilibrium points:
(i) $E_0(0, 0, \hat{P}, \hat{L})$ **(ii)** $E_1(\bar{F}, 0, \bar{P}, \bar{L})$ **(iii)** $E_2(0, \tilde{W}, \tilde{P}, \tilde{L})$ **(iv)** $E_3(F^*, W^*, P^*, L^*)$.

4.1 Existence of $E_0(0, 0, \hat{P}, \hat{L})$

Here, equilibrium values of $\hat{P}$ and $\hat{L}$ are obtained by solving following equations

$$\begin{aligned} &Q_0 - Q_1\hat{L} - \delta_0\hat{P} = 0 \\ &L_0 - \eta\hat{L} = 0. \end{aligned} \tag{3}$$

From the second equation of the system (3), we get

$$\hat{L} = \frac{L_0}{\eta}.$$

Substituting the above value of $\hat{L}$ in the first equation of system (3) , we have

$$\hat{P} = \frac{\eta Q_0 - Q_1 L_0}{\eta\delta_0}.$$

Clearly, $\hat{P}$ is positive if $(\eta Q_0 - Q_1 L_0) > 0$.
The inequality $\eta Q_0 > Q_1 L_0$ implies that ineffectiveness of lockdown should be large enough and implementation rate of lockdown should be small enough, for the existence of the equilibrium point $E_0(0, 0, \hat{P}, \hat{L})$.

4.2 Existence of $E_1(\bar{F}, 0, \bar{P}, \bar{L})$

In this case, equilibrium values of $\bar{F}$, $\bar{P}$ and $\bar{L}$ are obtained by solving following equations:

$$\begin{aligned} &r\left(1 - \frac{\bar{F}}{K}\right) - \pi_1\beta_1\bar{P} - h_{0_1} + e_1\bar{L} = 0 \\ &Q_0 - Q_1\bar{L} - \beta_1\bar{F}\bar{P} - \delta_0\bar{P} = 0 \\ &L_0 - \eta\bar{L} = 0. \end{aligned} \tag{4}$$

From the third equation of system (4), we have

$$\bar{L} = \frac{L_0}{\eta}.$$

Substituting the above value of $\bar{L}$ in the second equation of system (4), we get

$$\bar{P} = \frac{\eta Q_0 - Q_1 L_0}{\eta(\beta_1\bar{F} + \delta_0)} = f_1(\bar{F}), \text{ (say)}. \tag{5}$$

Now, we define a function

$$\phi_1(F) = r - \frac{rF}{K} - \pi_1\beta_1 f_1(F) - h_{0_1} + e_1\frac{L_0}{\eta}. \tag{6}$$

From (6), we get

$$\begin{aligned}\phi_1(0) &= r - \pi_1\beta_1 f_1(0) - h_{0_1} + e_1\frac{L_0}{\eta}\\ &= r - \pi_1\beta_1\left(\frac{\eta Q_0 - Q_1 L_0}{\eta\delta_0}\right) - h_{0_1} + e_1\frac{L_0}{\eta}\\ &= \left(r + e_1\frac{L_0}{\eta}\right) - \left(\pi_1\beta_1\left(\frac{\eta Q_0 - Q_1 L_0}{\eta\delta_0}\right) + h_{0_1}\right).\end{aligned}$$

Here, $\phi_1(0) > 0$, if

$$\left(r + e_1\frac{L_0}{\eta}\right) - \left(\pi_1\beta_1\left(\frac{\eta Q_0 - Q_1 L_0}{\eta\delta_0}\right) + h_{0_1}\right) > 0.$$

Again, from (6) we have

$$\begin{aligned}&\phi_1(F_{\max})\\ &= \left(r + e_1\frac{L_0}{\eta}\right) - \left(\frac{rF_{\max}}{K} + \pi_1\beta_1 f_1(F_{\max}) + h_{0_1}\right)\\ &= -\left(\pi_1\beta_1\left(\frac{\eta Q_0 - Q_1 L_0}{\eta(\beta_1 F_{\max} + \delta_0)}\right) + h_{0_1}\right).\end{aligned}$$

Thus, $\phi_1(F_{\max}) < 0$, by the existence of equilibrium point E_0.
Then, there exists a root $\bar{F}$ in the interval $0 < \bar{F} < F_{\max}$ such that

$$\phi_1(\bar{F}) = 0.$$

For the uniqueness of $\bar{F}$, the sufficient condition is $\frac{\mathrm{d}\phi_1}{\mathrm{d}F} < 0$ at $\bar{F}$, where

$$\begin{aligned}\frac{\mathrm{d}\phi_1}{\mathrm{d}F} &= -\frac{r}{K} - \pi_1\beta_1 f_1'(F)\\ &= -\frac{r}{K} + \pi_1\beta_1^2\left(\frac{\eta Q_0 - Q_1 L_0}{\eta(\beta_1 F + \delta_0)^2}\right).\end{aligned}$$

Therefore, $\frac{\mathrm{d}\phi_1}{\mathrm{d}F} < 0$ at $\bar{F}$, if

$$-\frac{r}{K} + \pi_1\beta_1^2\left(\frac{\eta Q_0 - Q_1 L_0}{\eta(\beta_1\bar{F} + \delta_0)^2}\right) < 0.$$

After knowing the value of $\bar{F}$, the value of $\bar{P}$ can be obtained by (5) which is positive by the existence of E_0.

4.3 Existence of $E_2(0, \tilde{W}, \tilde{P}, \tilde{L})$

In equilibrium $E_2(0, \tilde{W}, \tilde{P}, \tilde{L})$, $\tilde{W}$, $\tilde{P}$ and $\tilde{L}$ satisfy the following equations:

$$\begin{aligned}s\left(1 - \frac{\tilde{W}}{M}\right) - \beta_2\tilde{P} - h_{0_2} + e_2\tilde{L} &= 0\\ Q_0 - Q_1\tilde{L} + \pi_2\beta_2\tilde{W}\tilde{P} - \delta_0\tilde{P} &= 0\\ L_0 - \eta\tilde{L} &= 0.\end{aligned} \tag{7}$$

From the third equation of system (7), we get

$$\tilde{L} = \frac{L_0}{\eta}.$$

Substituting the above value of $\tilde{L}$ in the second equation of system (7), we get

$$\tilde{P} = \left(\frac{\eta Q_0 - Q_1 L_0}{\eta(\delta_0 - \pi_2\beta_2\tilde{W})}\right) = f_2(\tilde{W}), \text{ (say)}. \tag{8}$$

Now, we define a function

$$\phi_2(W) = s - \frac{sW}{M} - \beta_2 f_2(W) - h_{0_2} + e_2\frac{L_0}{\eta}. \tag{9}$$

From (9), we get

$$\begin{aligned}\phi_2(0) &= s - \beta_2 f_2(0) - h_{0_2} + e_2\frac{L_0}{\eta}\\ &= s - \beta_2\left(\frac{\eta Q_0 - Q_1 L_0}{\eta\delta_0}\right) - h_{0_2} + e_2\frac{L_0}{\eta}\\ &= \left(s + e_2\frac{L_0}{\eta}\right) - \left(\beta_2\left(\frac{\eta Q_0 - Q_1 L_0}{\eta\delta_0}\right) + h_{0_2}\right).\end{aligned}$$

Thus, $\phi_2(0) > 0$ if

$$\left(s + e_2\frac{L_0}{\eta}\right) - \left(\beta_2\left(\frac{\eta Q_0 - Q_1 L_0}{\eta\delta_0}\right) + h_{0_2}\right) > 0.$$

Again from (9), it is obtained that

$$\begin{aligned}&\phi_2(W_{\max})\\ &= \left(s + e_2\frac{L_0}{\eta}\right) - \left(\frac{sW_{\max}}{M} + \beta_2 f_2(W_{\max}) + h_{0_2}\right)\\ &= -\left(\alpha_2 F_{\max} + \beta_2\left(\frac{\eta Q_0 - Q_1 L_0}{\eta(\delta_0 - \pi_2\beta_2 W_{\max})}\right) + h_{0_2}\right).\end{aligned}$$

Therefore, $\phi_2(W_{\max}) < 0$, if

$$\left(\alpha_2 F_{\max} + \beta_2\left(\frac{\eta Q_0 - Q_1 L_0}{\eta(\delta_0 - \pi_2\beta_2 W_{\max})}\right) + h_{0_2}\right) > 0.$$

Then, there exists a root $\tilde{W}$ in the interval $0 < \tilde{W} < W_{\max}$ such that

$$\phi_2(\tilde{W}) = 0.$$

For the uniqueness of $\tilde{W}$, the sufficient condition is $\frac{\mathrm{d}\phi_2}{\mathrm{d}W} < 0$ at $\tilde{W}$, where

$$\frac{\mathrm{d}\phi_2}{\mathrm{d}W} = -\frac{s}{M} - \beta_2 f_2'(W) = -\left(\frac{s}{M} + \pi_2\beta_2^2\left(\frac{\eta Q_0 - Q_1 L_0}{\eta(\delta_0 - \pi_2\beta_2 W)^2}\right)\right).$$

Since $\frac{s}{M} + \pi_2\beta_2^2\left(\frac{\eta Q_0 - Q_1 L_0}{\eta(\delta_0 - \pi_2\beta_2\tilde{W})^2}\right) > 0$, therefore, $\frac{\mathrm{d}\phi_2}{\mathrm{d}W} < 0$ at $\tilde{W}$.
After knowing the value of $\tilde{W}$, the value of $\tilde{P}$ can be obtained by (8) which is positive if equilibrium point E_0 exists and $(\delta_0 - \pi_2\beta_2\tilde{W}) > 0$.

4.4 Existence of $E_3(F^*, W^*, P^*, L^*)$

In this case, equilibrium values of F^*, W^*, P^* and L^* are solutions of following equations:

$$\begin{aligned} r\left(1 - \frac{F^*}{K}\right) - \alpha_1 W^* - \pi_1\beta_1 P^* - h_{0_1} + e_1 L^* &= 0 \\ s\left(1 - \frac{W^*}{M}\right) + \alpha_2 F^* - \beta_2 P^* - h_{0_2} + e_2 L^* &= 0 \\ Q_0 - Q_1 L^* - \beta_1 F^* P^* + \pi_2\beta_2 W^* P^* - \delta_0 P^* &= 0 \\ L_0 - \eta L^* &= 0. \end{aligned} \tag{10}$$

From the fourth equation of system (10), we have

$$L^* = \frac{L_0}{\eta}. \tag{11}$$

Substituting the above value of L^* in the second equation of system (10), we get

$$W^* = \frac{M}{s}\left(s + \alpha_2 F^* - \beta_2 P^* - h_{0_2} + e_2\frac{L_0}{\eta}\right). \tag{12}$$

Using (11) and (12) in the first equation of system (10), it is obtained that

$$F^* = \left(\frac{r - \alpha_1 M + \left(\frac{\alpha_1\beta_2 M}{s} - \pi_1\beta_1\right)P^* + \frac{\alpha_1 M h_{0_2}}{s} - \frac{\alpha_1 e_2 M L_0}{\eta s} - h_{0_1} + e_1\frac{L_0}{\eta}}{\frac{\alpha_1\alpha_2 M}{s} + \frac{r}{K}}\right) = f_3(P^*), \text{ (say)}. \tag{13}$$

Equation (12) gives

$$\begin{aligned} W^* &= \frac{M}{s}\left(s + \alpha_2 f_3(P^*) - \beta_2 P^* - h_{0_2} + e_2\frac{L_0}{\eta}\right) \\ &= f_4(P^*), \text{ (say)}. \end{aligned} \tag{14}$$

For the existence of $E_3(F^*, W^*, P^*, L^*)$, we define a function

$$\begin{aligned} \phi_3(P) = Q_0 - Q_1\frac{L_0}{\eta} - \beta_1 f_3(P)P \\ +\pi_2\beta_2 f_4(P)P - \delta_0 P. \end{aligned} \tag{15}$$

From (15), we get

$$\phi_3(0) = \left(\frac{\eta Q_0 - Q_1 L_0}{\eta}\right).$$

Here, $\phi_3(0) > 0$, by the existence of equilibrium point E_0.

Again from (15), we note that

$$\begin{aligned} \phi_3(P_{\max}) &= Q_0 - Q_1\frac{L_0}{\eta} - \beta_1 f_3(P_{\max})P_{\max} \\ &\quad +\pi_2\beta_2 f_4(P_{\max})P_{\max} - \delta_0 P_{\max}, \\ &= \left(\frac{\eta Q_0 - Q_1 L_0}{\eta} + \pi_2\beta_2 f_4(P_{\max})P_{\max}\right) \\ &\quad -(\beta_1 f_3(P_{\max}) + \delta_0)P_{\max}. \end{aligned}$$

Therefore, $\phi_3(P_{\max}) < 0$ if

$$\left(\frac{\eta Q_0 - Q_1 L_0}{\eta} + \pi_2\beta_2 f_4(P_{\max})P_{\max}\right) - (\beta_1 f_3(P_{\max}) + \delta_0)P_{\max} < 0.$$

Then, there exists a root P^* in the interval $0 < P^* < P_{\max}$ such that

$$\phi_3(P^*) = 0.$$

For the uniqueness of P^*, the sufficient condition is $\frac{\mathrm{d}\phi_3}{\mathrm{d}P} < 0$ at P^*, where

$$\begin{aligned} \frac{\mathrm{d}\phi_3}{\mathrm{d}P} &= -\beta_1 f_3(P) - \beta_1 f_3'(P)P \\ &\quad +\pi_2\beta_2 f_4(P) + \pi_2\beta_2 f_4'(P)P - \delta_0 \end{aligned}$$

$$= \pi_2\beta_2 f_4(P) + \pi_2\beta_2 f_4^{'}(P)P - (\beta_1 f_3(P) + \beta_1 f_3^{'}(P)P + \delta_0)$$

Thus $\frac{d\phi_3}{dP} < 0$ at P^*, if

$$\pi_2\beta_2 f_4(P^*) + \pi_2\beta_2 f_4^{'}(P^*)P^* - (\beta_1 f_3(P^*) + \beta_1 f_3^{'}(P^*)P^* + \delta_0) < 0.$$

After knowing the value of P^*, values of F^* and W^* can be found by (13) and (14), respectively. Further, F^* and W^* are positive if $f_3(P^*) > 0$ and $f_4(P^*) > 0$, respectively.

5 Stability analysis

5.1 Local stability analysis

Local stability of any equilibrium point can be determined by finding the eigenvalues of variational matrix at that point. The variational matrix $V(E)$ of system (2) is given by

$$V(E) = \begin{bmatrix} a_{11} & -\alpha_1 F & -\pi_1\beta_1 F & e_1 F \\ \alpha_2 W & a_{22} & -\beta_2 W & e_2 W \\ -\beta_1 P & \pi_2\beta_2 P & \pi_2\beta_2 W - \beta_1 F - \delta_0 & -Q_1 \\ 0 & 0 & 0 & -\eta \end{bmatrix},$$

where

$$a_{11} = r\left(1 - \frac{2F}{K}\right) - \alpha_1 W - \pi_1\beta_1 P - h_{0_1} + e_1 L,$$

$$a_{22} = s\left(1 - \frac{2W}{M}\right) + \alpha_2 F - \beta_2 P - h_{0_2} + e_2 L.$$

The variational matrix $V(E)$ at E_0 reduces into

$$V(E_0) = \begin{bmatrix} r - \pi_1\beta_1\hat{P} - h_{0_1} + e_1\hat{L} & 0 & 0 & 0 \\ 0 & s - \beta_2\hat{P} - h_{0_2} + e_2\hat{L} & 0 & 0 \\ -\beta_1\hat{P} & \pi_2\beta_2\hat{P} & -\delta_0 & -Q_1 \\ 0 & 0 & 0 & -\eta \end{bmatrix}.$$

From $V(E_0)$, we note that two eigenvalues of $V(E_0)$ are $(r - \pi_1\beta_1\hat{P} - h_{0_1} + e_1\hat{L})$ and $(s - \beta_2\hat{P} - h_{0_2} + e_2\hat{L})$. Thus, E_0 is unstable in $F - W$ plane, provided that $r + e_1\hat{L} > \pi_1\beta_1\hat{P} + h_{0_1}$ and $s + e_2\hat{L} > \beta_2\hat{P} + h_{0_2}$. Other two eigenvalues of $V(E_0)$ are $-\delta_0$ and $-\eta$ which are always negative. Therefore, E_0 is asymptotically stable in $P - L$ plane.

The variational matrix $V(E)$ at E_1 is given by

$$V(E_1) = \begin{bmatrix} -\frac{r}{K}\bar{F} & -\alpha_1\bar{F} & -\pi_1\beta_1\bar{F} & e_1\bar{F} \\ 0 & s + \alpha_2\bar{F} - \beta_2\bar{P} - h_{0_2} + e_2\bar{L} & 0 & 0 \\ -\beta_1\bar{P} & \pi_2\beta_2\bar{P} & -\beta_1\bar{F} - \delta_0 & -Q_1 \\ 0 & 0 & 0 & -\eta \end{bmatrix}.$$

From $V(E_1)$, we note that one eigenvalue of $V(E_1)$ is $(s + \alpha_2\bar{F} - \beta_2\bar{P} - h_{0_2} + e_2\bar{L})$ and another eigenvalue is $-\eta$ which is always negative. However, by Gerschgorin's theorem [26], other two eigenvalues have negative real part if the following conditions hold:

$$\beta_1\bar{P} < \frac{r}{K}\bar{F}$$

$$\pi_1\beta_1\bar{F} < \beta_1\bar{F} + \delta_0$$

The second inequality can be written as $\beta_1\bar{F}(1-\pi_1)+\delta_0 > 0$, which obviously holds as $\pi_1 < 1$. Therefore, E_1 is stable in $F - P - L$ manifold, provided that $\beta_1\bar{P} < \frac{r}{K}\bar{F}$ and unstable along W-direction if $s + \alpha_2\bar{F} + e_2\bar{L} > \beta_2\bar{P} + h_{0_2}$.

The variational matrix $V(E)$ at E_2 is given by

$$V(E_2) = \begin{bmatrix} r - \alpha_1\tilde{W} - \pi_1\beta_1\tilde{P} - h_{0_1} + e_1\tilde{L} & 0 & 0 & 0 \\ \alpha_2\tilde{W} & -\frac{s}{M}\tilde{W} & -\beta_2\tilde{W} & e_2\tilde{W} \\ -\beta_1\tilde{P} & \pi_2\beta_2\tilde{P} & \pi_2\beta_2\tilde{W} - \delta_0 & -Q_1 \\ 0 & 0 & 0 & -\eta \end{bmatrix}.$$

From $V(E_2)$, we note that two eigenvalues are $(r - \alpha_1\tilde{W} - \pi_1\beta_1\tilde{P} - h_{0_1} + e_1\tilde{L})$ and $-\eta$. Other two eigenvalues $V(E_2)$ are roots of a quadratic equation, which are either negative or have negative real part. Therefore, E_2 is stable in $W - P - L$ manifold and unstable along F-direction if $r + e_1\tilde{L} > \alpha_1\tilde{W} + \pi_1\beta_1\tilde{P} + h_{0_1}$.

The variation matrix $V(E)$ at the interior equilibrium point E_3 reduces into

$$V(E_3) = \begin{bmatrix} -\frac{r}{K}F^* & -\alpha_1 F^* & -\pi_1\beta_1 F^* & e_1 F^* \\ \alpha_2 W^* & -\frac{s}{M}W^* & -\beta_2 W^* & e_2 W^* \\ -\beta_1 P^* & \pi_2\beta_2 P^* & -\left(\frac{Q_0 - Q_1 L^*}{P*}\right) & -Q_1 \\ 0 & 0 & 0 & -\eta \end{bmatrix}.$$

By Gerschgorin's theorem [26], all eigenvalues of variational matrix $V(E_3)$ have negative real part if following conditions are satisfied

$$\alpha_2 W^* + \beta_1 P^* < \frac{r}{K}F^*,$$

$$\alpha_1 F^* + \pi_2\beta_2 P^* < \frac{s}{M}W^*,$$

$$\pi_1\beta_1 F^* + \beta_2 W^* < \left(\frac{Q_0 - Q_1 L^*}{P*}\right),$$

$$e_1 F^* + e_2 W^* + Q_1 < \eta.$$

Therefore, E_3 is locally asymptotically stable under above conditions.

5.2 Global stability analysis

Theorem 5.1 *If the following inequalities hold:*

$$(\alpha_1 - m_1\alpha_2)^2 < \frac{4}{9}\frac{rs}{KM},$$
$$e_1^2 < \frac{4}{9}\frac{r\eta}{K},$$
$$m_1 e_2^2 < \frac{4}{9}\frac{s\eta}{M},$$

where $m_1 = \dfrac{\beta_1 F^* + \delta_0}{\pi_2\beta_2 W^*}$, *then equilibrium point* E_3 *is globally stable with respect to all solutions initiating in* Ω.

Proof Consider the following positive-definite function

$$S = \left(F - F^* - F^*\ln\frac{F}{F^*}\right) + m_1\left(W - W^* - W^*\ln\frac{W}{W^*}\right) + \frac{1}{2}(P - P^*)^2 + \frac{1}{2}(L - L^*)^2.$$

where m_1 is positive constant to be chosen appropriately. Now, differentiating S with respect to t, we get

$$\begin{aligned}\frac{\mathrm{d}S}{\mathrm{d}t} &= (F - F^*)\left[r - \frac{r}{K}F - \alpha_1 W - \pi_1\beta_1 P - h_{0_1} + e_1 L\right] \\ &+ m_1(W - W^*)\left[s - \frac{s}{M}W + \alpha_2 F - \beta_2 P - h_{0_2} + e_2 L\right] \\ &+ (P - P^*)\left[Q_0 - Q_1 L - \beta_1 F P + \pi_2\beta_2 W P - \delta_0 P\right] \\ &+ (L - L^*)\left[L_0 - \eta L\right].\end{aligned}$$

Using (10) and then after doing some algebraic manipulations, we have

$$\begin{aligned}\frac{\mathrm{d}S}{\mathrm{d}t} &= -\frac{1}{3}\frac{r}{K}(F - F^*)^2 - (\alpha_1 - m_1\alpha_2)(F - F^*)(W - W^*) \\ &-\frac{1}{3}\frac{s}{M}(W - W^*)^2 \\ &-\frac{1}{3}\frac{r}{K}(F - F^*)^2 - (\pi_1\beta_1 + \beta_1 P)(F - F^*)(P - P^*) \\ &-\frac{1}{3}(\beta_1 F^* - m_1\pi_2\beta_2 W^* + \delta_0)(P - P^*)^2 \\ &-\frac{1}{3}\frac{r}{K}(F - F^*)^2 + e_1(F - F^*)(L - L^*) \\ &-\frac{1}{3}\eta(L - L^*)^2 - \frac{1}{3}\frac{m_1 s}{M}(W - W^*)^2 \\ &-m_1(\beta_2 - \pi_2\beta_2 P)(W - W^*)(P - P^*) \\ &-\frac{1}{3}(\beta_1 F^* - m_1\pi_2\beta_2 W^* + \delta_0)(P - P^*)^2 \\ &-\frac{1}{3}\frac{s}{M}(W - W^*)^2 + m_1 e_2(W - W^*)(L - L^*) \\ &-\frac{1}{3}\eta(L - L^*)^2 - \frac{1}{3}(\beta_1 F^* - m_1\pi_2\beta_2 W^* + \delta_0) \\ &\times(P - P^*)^2 - Q_1(P - P^*)(L - L^*) - \frac{1}{3}\eta(L - L^*)^2.\end{aligned}$$

Selecting $m_1 = \dfrac{\beta_1 F^* + \delta_0}{\pi_2\beta_2 W^*}$, $\dfrac{\mathrm{d}S}{\mathrm{d}t}$ is negative definite if the following inequalities hold:

$$(\alpha_1 - m_1\alpha_2)^2 < \frac{4}{9}\frac{rs}{KM} \tag{16}$$
$$e_1^2 < \frac{4}{9}\frac{r\eta}{K} \tag{17}$$
$$m_1 e_2^2 < \frac{4}{9}\frac{s\eta}{M}. \tag{18}$$

Thus, S is Lyapunov function on Ω provided conditions (16)–(18) hold. This completes the proof of Theorem 5.1. □

6 Persistence

A population $F(t)$ of a system is said to be persistent if $F(t) > 0$ and $\liminf_{t\to\infty} F(t) > 0$ whenever $F(0) > 0$. Further, $F(t)$ is said to be uniformly persistent if $F(t)$ is persistent and $\exists\,\delta > 0$ (independent of $F(0)$) such that $\liminf_{t\to\infty} F(t) \geq \delta$. A system is said to be uniformly persistent if each component of the system persists uniformly.

Biologically, uniform persistence of a system means all of its population will survive in future.

Theorem 6.1 *System* (2) *persists uniformly if the following conditions hold:*

$$r - h_{0_1} > \alpha_1 W_{\max} + \pi_1\beta_1 P_{\max},$$
$$s - h_{0_2} > \beta_2 P_{\max} - \alpha_2 F_{\min},$$

and

$$\beta_1 F_{\max} - \pi_2\beta_2 W_{\min} + \delta_0 > 0,$$

where $F_{\min} = \dfrac{K}{r}(r - \alpha_1 W_{\max} - \pi_1\beta_1 P_{\max} - h_{0_1})$, $W_{\min} = \dfrac{M}{s}(s + \alpha_2 F_{\min} - \beta_2 P_{\max} - h_{0_2})$ *and* $P_{\min} = \left(\dfrac{Q_0 - Q_1 L_{\max}}{\beta_1 F_{\max} - \pi_2\beta_2 W_{\min} + \delta_0}\right)$.

Proof From the first equation of system (2), we get

$$\frac{\mathrm{d}F}{\mathrm{d}t} \geq F\left(r - \alpha_1 W_{\max} - \pi_1\beta_1 P_{\max} - h_{0_1} - \frac{r}{K}F\right).$$

This implies that,

$$\begin{aligned}\liminf_{t\to\infty} F(t) &\geq \frac{K}{r}(r-\alpha_1 W_{\max}-\pi_1\beta_1 P_{\max}-h_{0_1})\\ &= F_{\min}, \text{(say)}.\end{aligned}$$

Here, we note that $F_{\min} > 0$, if

$$r - h_{0_1} > \alpha_1 W_{\max} + \pi_1\beta_1 P_{\max}.$$

In a similar manner, the second equation of system (2) gives

$$\frac{\mathrm{d}W}{\mathrm{d}t} \geq W\left(s+\alpha_2 F_{\min}-\beta_2 P_{\max}-h_{0_2}-\frac{s}{M}W\right),$$

which implies that,

$$\begin{aligned}\liminf_{t\to\infty} W(t) &\geq \frac{M}{s}(s+\alpha_2 F_{\min}-\beta_2 P_{\max}-h_{0_2})\\ &= W_{\min}, \text{(say)}.\end{aligned}$$

Here, $W_{\min} > 0$, if

$$s - h_{0_2} > \beta_2 P_{\max} - \alpha_2 F_{\min}.$$

From the third equation of system (2), we have

$$\frac{\mathrm{d}P}{\mathrm{d}t} \geq Q_0 - Q_1 L_{\max} - (\beta_1 F_{\max} - \pi_2\beta_2 W_{\max} + \delta_0)P.$$

This implies that,

$$\begin{aligned}\liminf_{t\to\infty} P(t) &\geq \left(\frac{Q_0 - Q_1 L_{\max}}{\beta_1 F_{\max} - \pi_2\beta_2 W_{\min} + \delta_0}\right)\\ &= P_{\min}, \text{(say)}.\end{aligned}$$

Therefore, $P_{\min} > 0$, if equilibrium point E_0 exists and

$$\beta_1 F_{\max} - \pi_2\beta_2 W_{\min} + \delta_0 > 0.$$

From the fourth equation of system (2), we get

$$\frac{\mathrm{d}L}{\mathrm{d}t} \geq -\eta L.$$

This gives that,

$$\liminf_{t\to\infty} L(t) \geq 0 = L_{\min}, \text{(say)}.$$

Therefore, from above arguments and lemma 3.1, we have

$$\begin{aligned}F_{\min} \leq \liminf_{t\to\infty} F(t) \leq \limsup_{t\to\infty} F(t) \leq F_{\max},\\ W_{\min} \leq \liminf_{t\to\infty} W(t) \leq \limsup_{t\to\infty} W(t) \leq W_{\max},\\ P_{\min} \leq \liminf_{t\to\infty} P(t) \leq \limsup_{t\to\infty} P(t) \leq P_{\max},\\ L_{\min} \leq \liminf_{t\to\infty} L(t) \leq \limsup_{t\to\infty} L(t) \leq L_{\max}.\end{aligned}$$

Therefore, system (2) persists uniformly under the above inequalities. This completes the proof of Theorem 6.1. □

Remark 1 If harvesting rates of forestry biomass and wildlife species in the absence of lockdown are small and natural depletion rate coefficient of pollutants is high, then the system (2) persists uniformly. This illustrates the feasibility of our mathematical model.

7 Ecological interpretation of some key findings of local and global stability

Ecological interpretation of some key findings from the conditions of local as well as global stability reveals insight of results. From these conditions, we note that e_1, e_2 and Q_1 should be small and η should be large, which is ecologically feasible because e_1 and e_2 represent growth rates of forestry biomass and wildlife species due to lockdown, respectively, Q_1 represents depletion rate coefficient of pollutants due to increase in lockdown and η represents ineffectiveness of lockdown. Therefore, to establish local as well as the global stabilities of the interior equilibrium point, we observed that ineffectiveness of lockdown should be large enough and growth rates of forestry biomass and wildlife species due to lockdown as well as depletion rate coefficient of pollutants due to increase in lockdown should be small. This demonstrates the feasibility of our mathematical model as lockdown is not very effective on broad scale and cannot be implemented for long time.

8 Local bifurcation analysis

8.1 Transcritical bifurcation between E_2 and E_3

From the eigenvalue $r - \alpha_1\tilde{W} - \pi_1\beta_1\tilde{P} - h_{0_1} + e_1\tilde{L}$ of $V(E_2)$, it can be observed that the stability of E_2 depends on the parameter r. Also, from the first equation of (10), we can see that

$$F^* = \frac{K}{r}(r - \alpha_1 W^* - \pi_1\beta_1 P^* - h_{0_1} + e_1 L^*)$$

This shows that the interior equilibrium point exists if $r > \alpha_1 W^* + \pi_1\beta_1 P^* + h_{0_1} - e_1 L^*$. Therefore, we can observe that the stability of E_2 and existence of E_3 are interconnected and depend on the parameter r. For small values of r, the equilibrium point E_2 is stable but as r crosses a threshold value $r^* = \alpha_1\tilde{W} + \pi_1\beta_1\tilde{P} + h_{0_1} - e_1\tilde{L}$, the equilibrium point E_2 becomes unstable. Also, if $r = \alpha_1\tilde{W} + \pi_1\beta_1\tilde{P} + h_{0_1} - e_1\tilde{L}$, one eigenvalue of $V(E_2)$ is zero and other three

eigenvalues are negative. This shows that if we consider r as bifurcating parameter, transcritical bifurcation can exist between the equilibrium points E_2 and E_3.

9 Optimal control model

The implementation of lockdown is useful to decrease the concentration of pollutants, but the cost of implementation prevents them from being implemented on broad scale. As a result, implementation strategies that reduce the concentration of pollutants as well as the cost of implementation are preferred. For this, we have chosen the implementation rate of lockdown (i.e. L_0) as a control parameter in the model system (2). On a finite interval $[0\ t_f]$, Lebesgue-measurable functions $u(t)$ reflect the parameter L_0. Our goal is to minimize total cost functional J, which is provided by:

$$J = \int_0^{t_f} (AP(t) + Bu^2(t))\mathrm{d}t, \tag{19}$$

subject to

$$\begin{aligned}
\frac{\mathrm{d}F}{\mathrm{d}t} &= rF\left(1-\frac{F}{K}\right) - \alpha_1 WF - \pi_1\beta_1 FP - h_1(L)F,\\
\frac{\mathrm{d}W}{\mathrm{d}t} &= sW\left(1-\frac{W}{M}\right) + \alpha_2 WF - \beta_2 WP - h_2(L)W,\\
\frac{\mathrm{d}P}{\mathrm{d}t} &= Q(L) - \beta_1 FP + \pi_2\beta_2 WP - \delta_0 P,\\
\frac{\mathrm{d}L}{\mathrm{d}t} &= u(t) - \eta L,
\end{aligned} \tag{20}$$

where $F(0) \geq 0$, $W(0) \geq 0$, $P(0) > 0$, $L(0) \geq 0$, $h_1(L) = h_{0_1} - e_1 L$, $h_2(L) = h_{0_2} - e_2 L$ and $Q(L) = Q_0 - Q_1 L$. Here, the quantities A and B are positive weight parameters that balance the size of terms in an objective functional. We figure out the optimal control $u^*(t)$ so that

$$J\left(u^*(t)\right) = \min_{u(t)\in X} J\left(u(t)\right), \tag{21}$$

where control set is defined as $X = \{u(t)\colon u(t)$ is measurable and $0 \leq u(t) \leq u_{max}$ for $t \in [0, t_f]\}$.

Theorem 9.1 *There exists an optimal control u^* such that*

$$J\left(u^*(t)\right) = \min_{u(t)\in X} J\left(u(t)\right), \tag{22}$$

associated with the system of differential equations (20) with nonnegative initial conditions.

Proof Using a result in Lukes [27], the existence of a solution to the system (20) is assured because the solutions are bounded on finite-time intervals. The set X is a closed and convex set. Also, the integrand of the functional (19) is convex on X. In system (20), the right side of the equations is bounded by a linear control and state. In addition, $c_1 > 0$, $c_2 > 0$ and $q > 1$ exist, such that

$$AP(t) + Bu^2(t) \geq c_1(|u(t)|)^q - c_2. \tag{23}$$

Therefore, the existence of optimal control is guaranteed, using Fleming and Rishel's [28] result (Theorem 4.1, pp. 68-69). The Hamiltonian at time t is defined as:

$$\begin{aligned}
&H(F, W, P, L, u_1, u_2, u_3, u_4) = AP(t) + Bu^2(t)\\
&+ u_1\left[rF\left(1-\frac{F}{K}\right) - \alpha_1 WF - \pi_1\beta_1 FP - h_1(L)F\right]\\
&+ u_2\left[sW\left(1-\frac{W}{M}\right) + \alpha_2 WF - \beta_2 WP - h_2(L)W\right]\\
&+ u_3[Q(L) - \beta_1 FP + \pi_2\beta_2 WP - \delta_0 P] + u_4[u(t) - \eta L],
\end{aligned}$$

where $u_i (i = 1, 2, 3, 4)$ are adjoint variables at time t. The adjoint variables can be determined from the following system of equations:

$$\begin{aligned}
\dot{u}_1 &= -\frac{\partial H}{\partial F} = u_3\beta_1 P - u_2\alpha_2 W - u_1\left[r\left(1-\frac{2F}{K}\right)\right.\\
&\left.-\alpha_1 W - \pi_1\beta_1 P - (h_{01} - e_1 L)\right],\\
\dot{u}_2 &= -\frac{\partial H}{\partial W} = u_1\alpha_1 F - u_2\left[s\left(1-\frac{2W}{M}\right)\right.\\
&\left.+\alpha_2 F - \beta_2 P - (h_{02} - e_2 L)\right] - u_3\pi_2\beta_2 P,\\
\dot{u}_3 &= -\frac{\partial H}{\partial P} = -A + u_1\pi_1\beta_1 F + u_2\beta_2 W\\
&-u_3(\pi_2\beta_2 W - \delta_0 - \beta_1 F),\\
\dot{u}_4 &= -\frac{\partial H}{\partial L}\\
&= u_3 Q_1 + u_4\eta - u_1 e_1 F - u_2 e_2 W.
\end{aligned} \tag{24}$$

The transversality conditions are $u_1(t_f) = u_2(t_f) = u_3(t_f) = u_4(t_f) = 0$.

With the help of optimality condition, i.e. $\dfrac{\partial H}{\partial u} = 0$, we have $u(t) = -\dfrac{u_4}{2B}$.

Then, the optimal controls $u^*(t)$ are given as:

$$u^*(t) = \begin{cases} 0, & if \quad -\dfrac{u_4}{2B} \leq 0,\\ -\dfrac{u_4}{2B}, & if \quad 0 < -\dfrac{u_4}{2B} < u_{\max},\\ u_{\max}, & if \quad -\dfrac{u_4}{2B} \geq u_{\max}. \end{cases} \tag{25}$$

As a result, the characterization of optimum control $u^*(t)$, which minimizes J across the set X when applied to a state system, is provided by

$$u^*(t) = \max\left\{\min\left(-\frac{u_4}{2B}, u_{\max}, 0\right)\right\}. \tag{26}$$

The optimality system comprises the control system (20), the adjoint system (24), optimal control (26) and transversally conditions. □

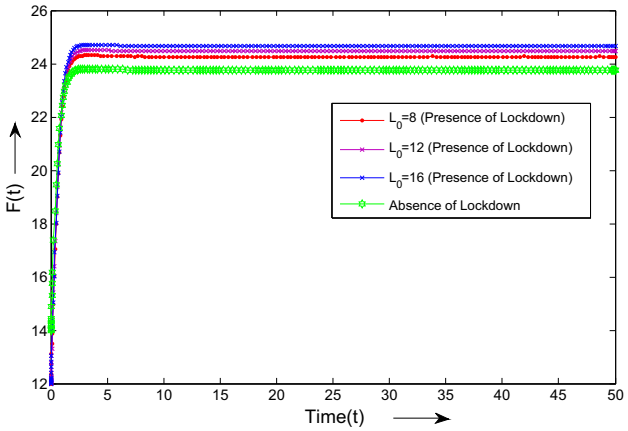

Fig. 1 Graph of F against t for different values of L_0

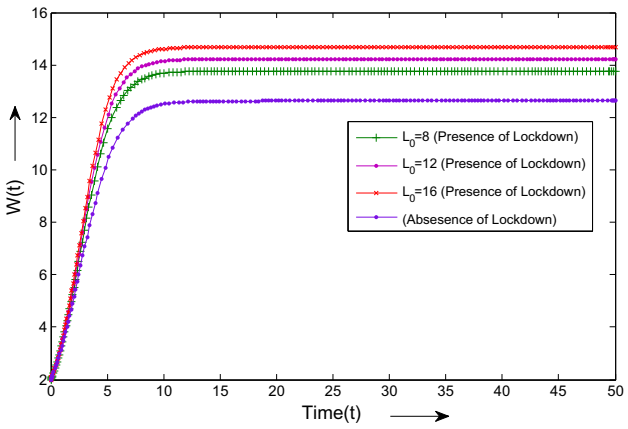

Fig. 2 Graph of W against t for different values of L_0

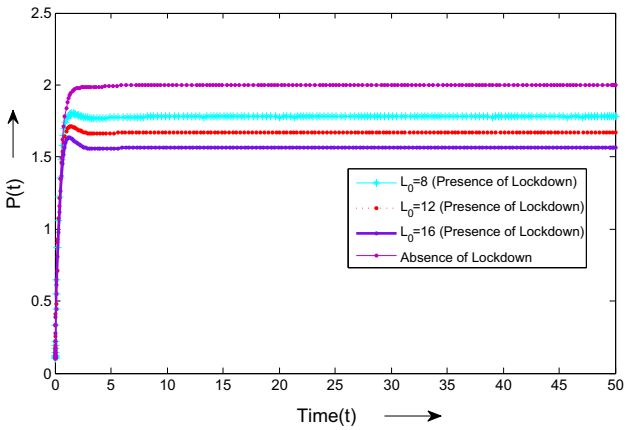

Fig. 3 Graph of P against t for different values of L_0

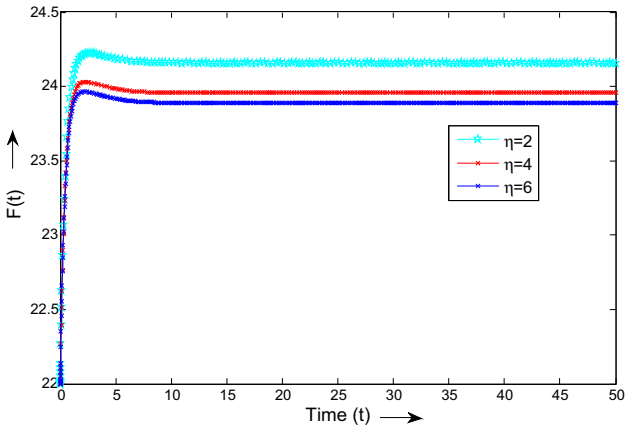

Fig. 4 Graph of F against t for different values of η

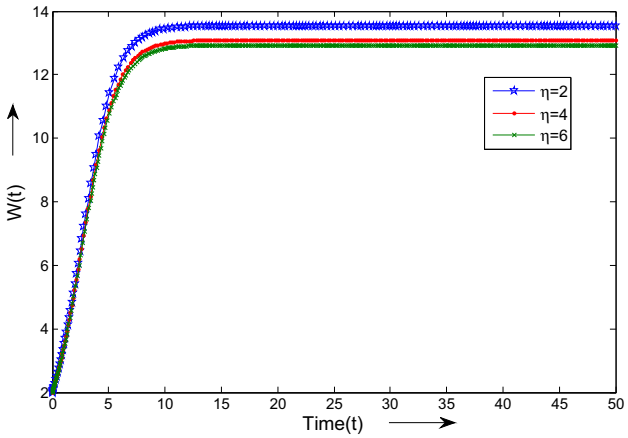

Fig. 5 Graph of W against t for different values of η

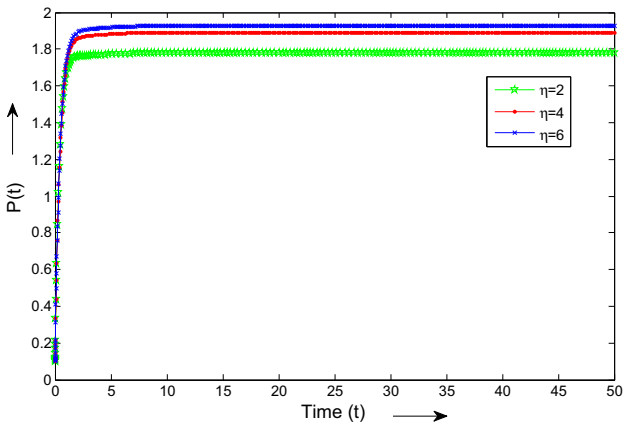

Fig. 6 Graph of P against t for different values of η

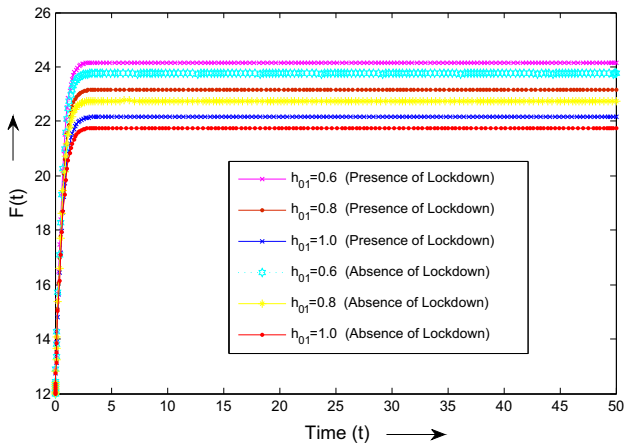

Fig. 7 Graph of F against t for different values of h_{0_1}

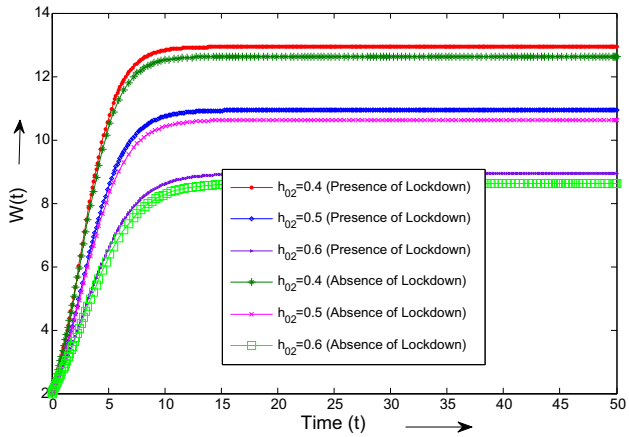

Fig. 8 Graph of W against t for different values of h_{0_2}

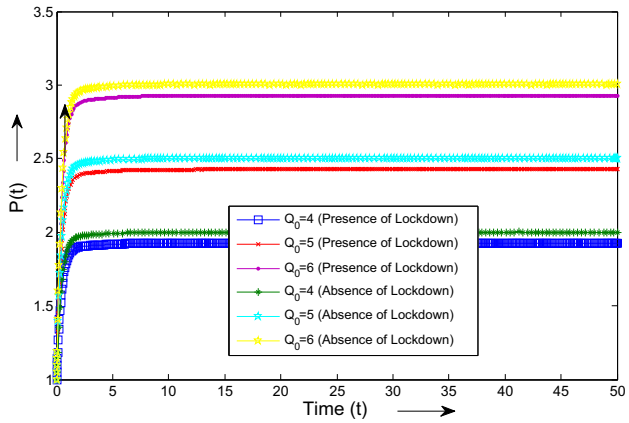

Fig. 9 Graph of P against t for different values of Q_0

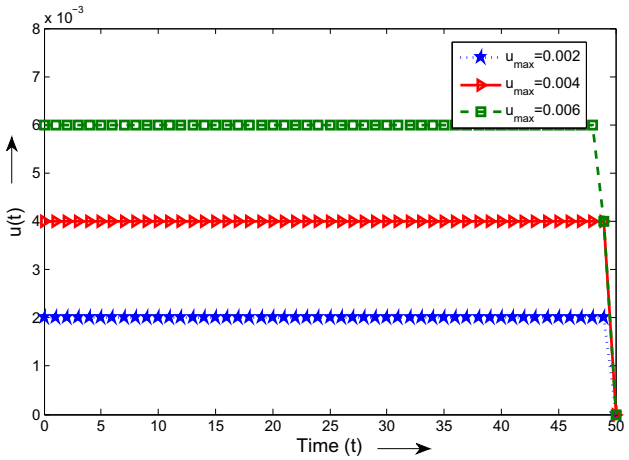

Fig. 10 Profile of $u(t)$ with respect to time t for different values of the maximum implementation rate ($u_{\max}$)

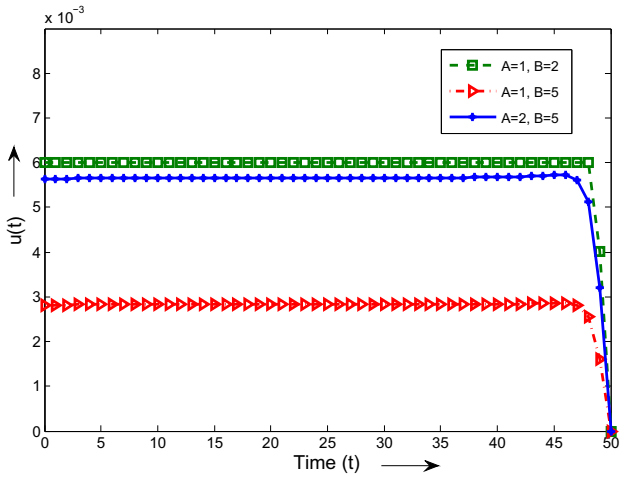

Fig. 11 Profile of $u(t)$ with respect to time t for different values of the weights A and B

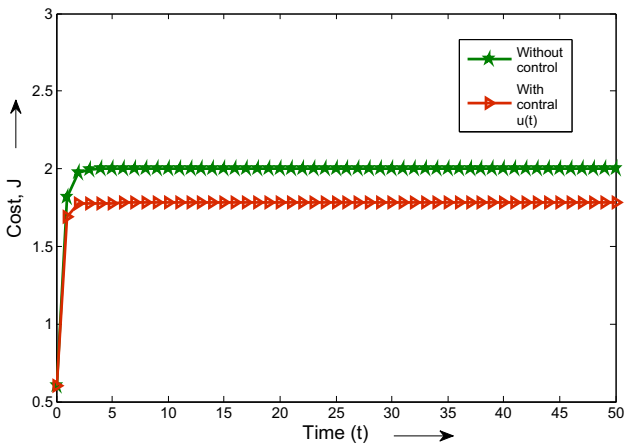

Fig. 12 Variation of cost function with respect to time t with and without control $u(t)$

10 Numerical simulations

To visualize our mathematical findings, some numerical simulations have been performed. For this, we choose the following set of parameter values

$$\begin{aligned} &r = 3, K = 30, \alpha_1 = 0.01, \pi_1 = 0.1, \beta_1 = 0.06, \\ &h_{0_1} = 0.6, e_1 = 0.01, s = 1, M = 20, \alpha_2 = 0.03, \\ &\pi_2 = 0.1, \beta_2 = 0.03, h_{0_2} = 0.4, e_2 = 0.01, Q_0 = 4, \\ &Q_1 = 0.1, \delta_0 = 0.6, L_0 = 8, \eta = 2. \end{aligned} \tag{27}$$

For the above set of parameters, the interior equilibrium point exists uniquely which is given by

$$\begin{aligned} &F^* = 24.1647, \quad W^* = 12.8602, \\ &P^* = 1.7785, \quad L^* = 4.000. \end{aligned}$$

Here, we note that all conditions of local stability, global stability and persistence of the interior equilibrium point are satisfied by set of parameters given in (27). The main aim of this paper is to see the impacts of lockdown on forestry biomass, wildlife species and pollution. Therefore, firstly we accentuate on the parameters and factors affecting lockdown. Figures 1 and 2 represent variations in the densities of forestry biomass and wildlife species with respect to t for different values of the implementation rate of lockdown (L_0), respectively. From these figures, it can be observed that the increase in the value of L_0 increases the equilibrium values of F and W, respectively. It depicts that the increased implementation rate of lockdown positively affects forestry biomass and wildlife species bot. From these figures, we can also infer that the absence of lockdown decreases the equilibrium values of F and W.

In Fig. 3, the concentration of pollutants is plotted against t for different values of the implementation rate of lockdown, L_0. This figure shows that the increase in the implementation rate of lockdown decreases the concentration of pollutants in the environment. Here, we also noted that the absence of lockdown increases the equilibrium level of P.

In Figs. 4 and 5, the densities of forestry biomass and wildlife species are plotted against time t for different values of η (rate of ineffectiveness of lockdown), respectively. These figures reveal that the increase in the value of η decreases the equilibrium levels of F and W. Here, it is noted that if we increase the value of η from 2 to 4, then there is a noticeable change in the levels of F and W but there is very slight change in the levels of F and W if we increase η from 4 to 6.

Figure 6 is the plot for P against time t for different values of η (rate of ineffectiveness of lockdown). This figure shows that increasing value of η increases the level of P. Here, we observe that if we increase the value of η from 2 to 4, then change in the levels of P is quite considerable, while if we increase η from 4 to 6, then there is a very moderate change in the levels of P.

Figure 7 is the plot for F against t for different values of $h_{0_1} = (0.6, 0.7, 0.8)$. This figure shows that the quantitative behaviour of F for increasing values of h_{0_1} is different in the presence and absence of lockdown. Here, it is noted that if the harvesting rate of forestry biomass is increasing and we impose lockdown, then the equilibrium level of F can be maintained.

In Fig. 8 , variations in W are plotted with respect to t for different values of $h_{0_2} = (0.4, 0.5, 0.6)$. Here, we observe that, in the presence and absence of lockdown the quantitative behaviour of W for increasing values of h_{0_2} is different. It depicts that if the wildlife harvest rate increases and lockdown is implemented, then the equilibrium level of W can be maintained.

Figure 9 is the plot of P against t for different values of $Q_0 = (4, 5, 6)$. It shows that the quantitative behaviour of P for increasing values of Q_0 differs in the presence and absence of lockdown. Here, it is noted that, for increasing emission rate of pollutants, the presence of lockdown decreases the equilibrium level of P. Therefore, the equilibrium level of P can be maintained by implementation of lockdown.

The optimality system, which consists of the control system (20), adjoint system (24), optimal control (26) and transversally criteria, is numerically integrated for the set of values given in equation (27) to indicate the optimum implementation scenario (20). Figure 10 is the plot of the optimal control profile $u(t)$ against t for different values of $u_{\max}$. As the value of the maximum implementation rate $u_{\max}$ increases, the time span over which lockdown efforts are implemented at their maximum rate decreases.

Figure 11 is the plot of the optimal control profile $u(t)$ against t for different values of weights A and B. With an increase in B, the time span over that lockdown efforts are executed at maximum rate decreases, whereas it increases with an increase in A. If the weight of the cost of implementing lockdown efforts is large, the efforts are applied at their higher rate for a shorter period of time and then reduced afterwards.

In addition, we conducted a cost design study to determine the most effective control mechanisms to use in Fig. 12. The cost of using control measures differs from the cost of not using control measures, as shown in this graph. Therefore, we recommend that control measures be implemented for sufficient period of time, as this will reduce the impact of the concentration of pollutants.

For the above set of parameters, trajectories with different initial conditions are drawn in Figs. 13, 14 and 15. From these figures, it can be seen that all trajectories with different initial points converges to same equilibrium point. Therefore, the interior equilibrium point is globally stable.

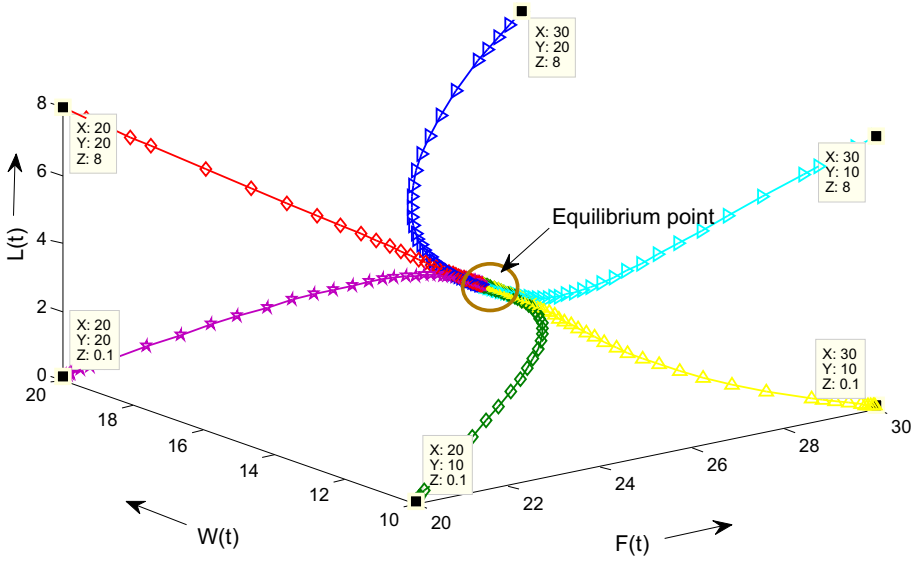

Fig. 13 Graph of $F - W - L$ for different initial starts

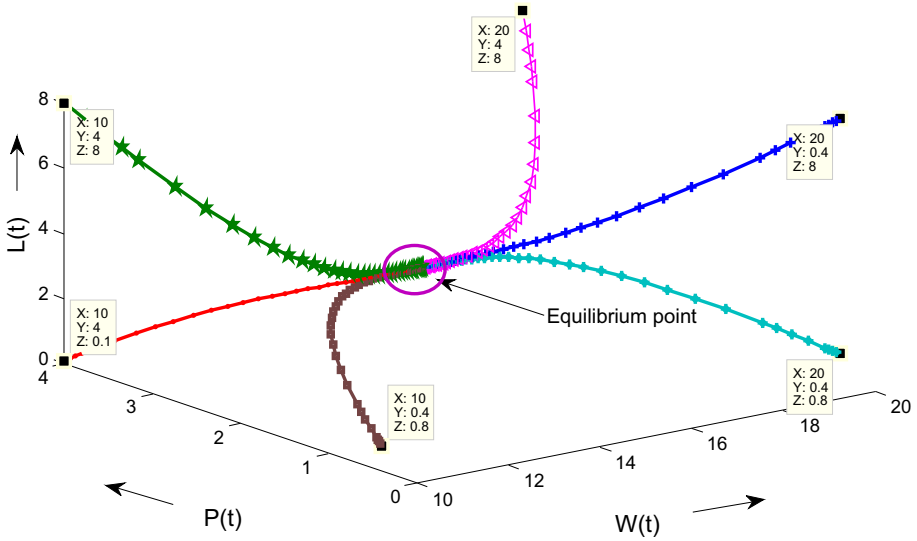

Fig. 14 Graph of $W - P - L$ for different initial starts

Figures 16, 17 and 18 are the plots of F, W and P against t for different values of r. Graph of L against t is not plotted for different values of r here, equilibrium value of L does not depend r, and we do not plot L. These figures depict that for small values of $r \leq r^*$, equilibrium point E_2 is stable. As value of r increases and crosses its threshold value $r^* = 0.6067$, equilibrium point E_2 loses its stability and the interior equilibrium point E_3 emanates. This shows that transcritical bifurcation occurs between equilibrium points E_2 and E_4 for threshold value $r^* = 0.6067$.

11 Conclusion

In this paper, a mathematical model to see the impacts of lockdown on the dynamics of both forestry biomass, wildlife species and control of atmospheric pollution has been formulated and analysed. Equilibrium analysis revealed that four equilibrium points exist for system (2). Conditions of local stability as well as global stability of the interior equilibrium point and persistence of system (2) have been obtained. By formulating an optimal control problem, the optimal strategies for minimizing the cost of implementation of lockdown as well as the concentration of pollutants have also been studied. We looked at the optimal control problem by plotting the implementation rate of lockdown as a function of time t. The optimal control theory was used to determine the characterization of the control parameter. The optimality problem is numerically solved, and the best strategies are presented. After performing numerical simulations, we have noted following results:

- Presence of lockdown increases the equilibrium levels of the densities of forestry biomass and wildlife species

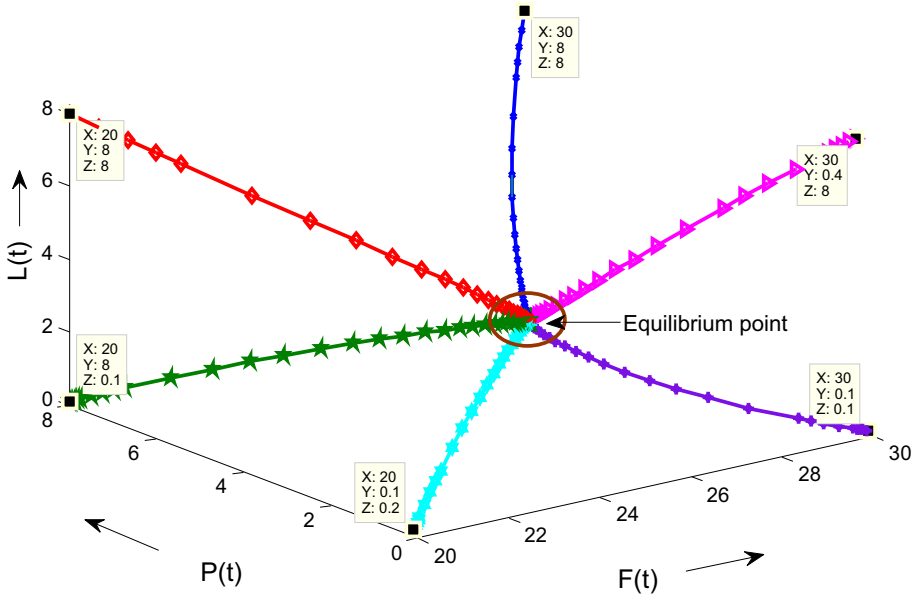

Fig. 15 Graph of $F - P - L$ for different initial starts

both and as rate of implementation of lockdown increases the densities of forestry biomass and wildlife species increases (Figs. 1 and 2).

- As rate of implementation of lockdown increases, the concentration of pollutants decreases (Fig. 3).
- There is noticeable increase in the densities of forestry biomass and wildlife species for small values of the rate of ineffectiveness of lockdown, but larger values are not much effective (Figs. 4 and 5).
- Small values of the rate of ineffectiveness of lockdown decreases P considerably but larger values are not much effective in controlling P (Fig. 6).
- The densities of forestry biomass and wildlife species decrease for increasing harvesting rate of forestry biomass and wildlife species, respectively, but these decreases can be maintained by implementing lockdown (Figs. 7 and 8).
- As emission rate of pollutants increases, the concentration of pollutants increases but this increase can be reduced by imposing lockdown (Fig. 9).
- Optimal control model (20) reveals that under the optimal scenario, the burden of pollutant's concentration is reduced. On the optimal profile of the implementation rate, the effect of modifications in the maximum implementation rate of lockdown and weight constants is noticed. As the value of the maximum implementation rate u_{max} increases, the time span over which lockdown efforts are implemented decreases. In the optimal sce-

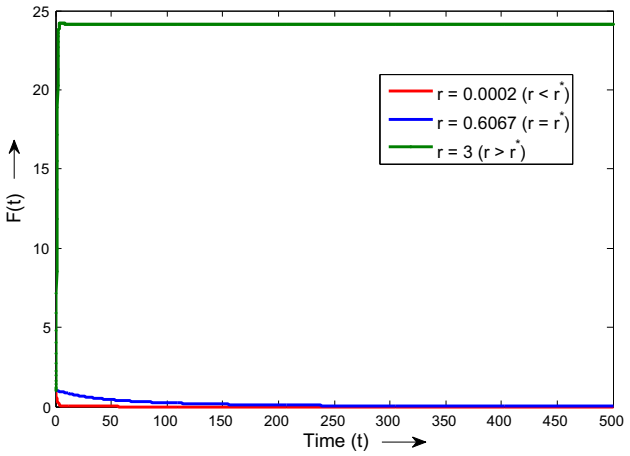

Fig. 16 Graph of F against t for different values of r illustrating convergence at equilibrium E_2 for $r \leq r^*$ and convergence at equilibrium E_3 for $r > r^*$

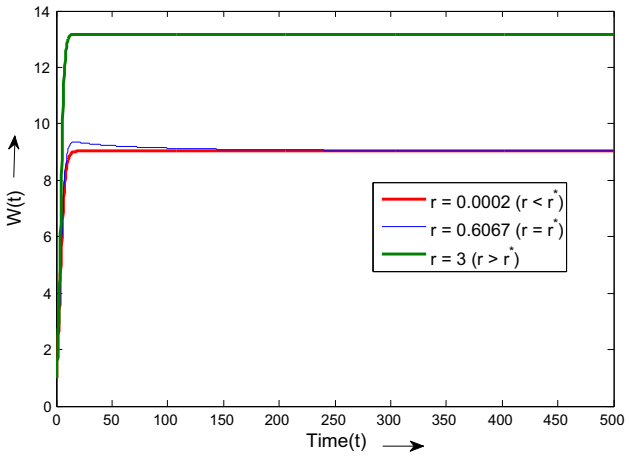

Fig. 17 Graph of W against t for different values of r illustrating convergence at equilibrium E_2 for $r \leq r^*$ and convergence at equilibrium E_3 for $r > r^*$

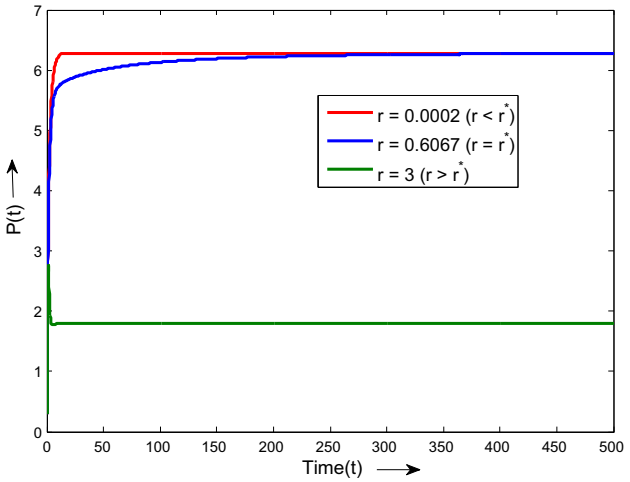

Fig. 18 Graph of P against t for different values of r illustrating convergence at equilibrium E_2 for $r \leq r^*$ and convergence at equilibrium E_3 for $r > r^*$

nario, the time span during which lockdown attempts are conducted at maximum rate decreases as the weights A and B of cost of implementation rate of lockdown decreases and increases, respectively (Figs. 10 and 11).

- The cost functional has different behaviour in the presence and absence of control. Presence of control measure decreases the cost functional (Fig. 12).

Therefore, to tackle the problem of excessive harvesting of both forestry biomass and wildlife species and increasing concentration of pollutants in the environment, implementation of lockdown will definitely work. It is also found that lockdown policy is effective in the optimal control of atmospheric pollution.

Declarations

Conflict of interest The authors declare that they do not have any conflict of interest.

References

1. "Lockdown" Wikipedia, The Free Encyclopedia https://en.wikipedia.org/wiki/Lockdown (accessed May 6, 2021)
2. Wang M, Liu F, Zheng M (2020) Air quality improvement from COVID-19 lockdown: evidence from China. Air Qual Atmos Health 1–14
3. Lokhandwala S, Gautam P (2020) Indirect impact of COVID-19 on environment: a brief study in Indian context. Environ Res 188:109807
4. Vogt Kristina A et al (2006) Global societies and forest legacies creating today's forest landscapes, Forests and society: sustainability and life cycles of forests in human landscapes, pp 30–59
5. Adams EA (2012) World forest area still on the decline, Earth Policy Institute, Europe 989.998 1-5. www.earth-policy.org/indicators/C56
6. World Bank Open Data (WBOD) (2020) Forest area (sq. km). https://data.worldbank.org/indicator/AG.LND.FRST.K2
7. Food and Agriculture Organization (FAO) (2015) Global forest resources assessment 2015: Main Report. http://www.fao.org/forest-resources-assessment/past-assessments/fra-2015/en/
8. Dubey B, Sharma S, Sinha P, Shukla JB (2009) Modelling the depletion of forestry resources by population and population pressure augmented industrialization. Appl Math Model 33(7):3002–3014
9. Agarwal M, Fatima T, Freedman HI (2010) Depletion of forestry resource biomass due to industrialization pressure: a ratio-dependent mathematical model. J Biol Dyn 4(4):381–396
10. Shukla JB, Dubey B (1997) Modelling the depletion and conservation of forestry resources: effects of population and pollution. J Math Biol 36(1):71–94
11. Shukla JB, Lata K, Misra AK (2011) Modeling the depletion of a renewable resources by population and industrialisation: effect of technology on its conservation. Nat Resour Model 24(2):242–267
12. Devi S, Gupta N (2019) A Mathematical model to analyze the dependence of biomass on the concentration of CO_2. Int J Ecol Dev 34(1):15–24
13. Devi S, Gupta N (2019) Dynamics of carbon dioxide gas (CO_2): effects of varying capability of plants to absorb CO_2. Nat Resour Model 32(1):e12174
14. Agarwal M, Devi S (2011) Harvesting of the vegetation biomass and grazer population with its effects on predator population: a mathematical model. Int J Ecol Econ Stat 20
15. Devi S (2012) Nonconstant prey harvesting in ratio-dependent predator–prey system incorporating a constant prey refuge. Int J Biomath 5(02):1250021
16. Devi S, Gupta N (2018) Logistic growth vs regrowth model with delay for the harvesting of vegetation biomass with its effects on CO_2. Nonlinear Stud 25(2)
17. Mondal B, Ghosh U, Rahman MS, Saha P, Sarkar S (2022) Studies of different types of bifurcations analyses of an imprecise two species food chain model with fear effect and non-linear harvesting. Math Comput Simul 192:111–135
18. Majumdar P, Debnath S, Mondal B, Sarkar S, Ghosh U (2022) Complex dynamics of a prey-predator interaction model with Holling type-II functional response incorporating the effect of fear on prey and non-linear predator harvesting. Rendiconti del Circolo Matematico di Palermo Series 2:1–32
19. Yuan R, Jiang W, Wang Y (2015) Saddle-node-Hopf bifurcation in a modified Leslie–Gower predator–prey model with time-delay and prey harvesting. J Math Anal Appl 422(2):1072–1090
20. Mondal B, Roy S, Ghosh U, Tiwari PK (2022) A systematic study of autonomous and nonautonomous predator–prey models for the combined effects of fear, refuge, cooperation and harvesting. Eur Phys J Plus 137(6):724
21. Dubey B, Das B (1999) Models for the survival of species dependent on resource in industrial environment. J Math Anal Appl 231(2):374–396
22. Freedman HI, Shukla JB (1991) Models for the effects of toxicant in single-species and predator–prey systems. J Math Biol 30(1):15–30
23. Shukla JB, Sharma S, Dubey B, Sinha P (2009) Modeling the survival of aresource-dependent population: effects of toxicants (pollutants) emitted from external sources as well as formed by its precursors. Nonlinear Anal Real World Appl 10(1):54–70
24. Misra AK, Verma M, Venturino E (2015) Modeling the control of atmospheric carbon dioxide through reforestation: effect of time delay. Model Earth Syst Environ 1(3):1–17

25. Verma M, Verma AK (2021) Effect of plantation of genetically modified trees on the control of atmospheric carbon dioxide: a modeling study. Nat Resour Model 34(2):e12300
26. Lancaster PL, Tismenetsky M (1985) The theory of matrices, second ed. Academic Press, New York, 371
27. Lukes DL (1982) Differential equations: classical to controlled. Academic Press, Edinburgh
28. Fleming WH, Rishel RW (2012) Deterministic and stochastic optimal control (Vol. 1) Springer Science and Business Media